J. Appl. Environ. Biol. Sci., 7(2)18-32, 2017

ISSN: 2090-4274
Journal of Applied Environmental and Biological Sciences
www.textroad.com

Direct Particle Fate Simulation in Electro- Static Precipitator (ESP) Process by a Full Finite Difference Scheme: A Formulation for ESP Efficiency in Particulate Matter Removal

A. Jafarimoghaddam[1*], S. Aberoumand[2], A. Taheri[3]

[1*]Department of Aerospace Engineering, K. N. Toosi University of Technology, Tehran, Iran
[3]Young Researchers and Elite Club, Takestan Branch, Islamic Azad University, Takestan, Iran
[3]Department of Civil Engineering, Sharif University of Technology, Tehran, Iran

Received: October 24, 2016
Accepted: December 15, 2016

ABSTRACT

The present work provides a numerical simulation of a wire- plate electrostatic precipitator. Considering that the previous aerosol works proved that the turbulence phenomenon is an effective parameter on particles motion, in this study the simulation was continued by employing k-ε turbulent model using a Finite Difference approach. Corona plasma was solved by an explicit FTCD (Forward Time, Central Distance) iterative model which is briefly introduced through this paper. Then, the electrostatic solution was implemented into the flow momentum equations as the source term. The definition of particle charge allowed us to track the particles with respect to the simplified particle trajectory equation. A simple dynamic tracking scheme was used to track a finite number of particles inside the ESP channel to their fates. Although there were some simplifications/ limitations in the present numerical simulation, but the outcome results were in a good agreement with the previous works in this field. Therefore, by the present work, it is insisted that a careful ESP simulation by direct particles tracking scheme may be considered as an alternative to more traditional approaches as at least the simulation procedure is much faster. Finally, a formulation is proposed for ESP efficiency in removing the particulate matters as a function of the number of applied wires and their average distance from the inlet of the ESP channel. This formulation could be beneficial for primary calculations in industrialization of ESP.
KEYWORDS: Aerosol, Corona Plasma, Finite Difference Method (FDM), ESP, Particle Tracking

INTRODUCTION

Before industrializing an ESP, because of the high costs for providing a full ESP setup, it is much worth to model the problem by CFD simulation and the value of numerical simulations has been proved over the decades. So the present work, aims to employ CFD for proceeding with ESP simulation. Although a real ESP is a three dimensional phenomenon, but, ignoring three dimensional releasing effect allows one to consider an ESP as a two dimensional problem and regarding this, there are lots of 2D simulations of Electro- Static Precipitator in the literature [see 1- 5]. Before 2007, most of the ESP simulations were conducted assuming a single electric wire (even if the real ESP contained more than one ionic wind wire); Multi- wired ESPs were then fully simulated in later studies[6- 8] to produce a complete consideration of the ESP problem. However, almost, all the previous studies in this field have been carried out dealing with Eulerian parameters. Dealing with Eulerian parameters such as concentration, takes us far from a comprehensive understanding of particles motion in individual; while having a full Lagrangian particle tracking, may provide a better understanding of the complex phenomena through the ESP problem such as Brownian motions of the many particles, absorption of particles by impacting to each other and etc. In the present work it is shown how particles behave individually through the ESP. Although there are some simplifications in the new model presented in this work, but yet this particle tracking model can provide us with some more details of ESP problem. Furthermore, this simplified scheme can be considered as an alternative to more traditional approaches to simulating ESP. As previously mentioned, first, the corona plasma wind was solved by an explicit approach to the coupled equations of electric field and charge transport. Then the solution is implemented into Reynolds Average Navier- Stokes equation. k-ε turbulent model was taken into account to capture the turbulent eddy- viscosity which is supposed to represent the impact of unresolved velocity fluctuations. Then, focusing on tracking ash particles through the aerosol process of the modeled ESP, the simplified equation of particle trajectory was solved with a simple algorithm for a finite number of particles. It was seen that the results for collected ash

***Corresponding Author:** A. Jafarimoghaddam, Department of Aerospace Engineering, K. N. Toosi University of Technology, Tehran, Iran Email Address: a.jafarimoghaddam@gmail.com; Phone No.:(+98) 9356651957

particles via grounded plates were in a good agreement with the previous works in the literature. Finally, based on the results of the numerical simulation, a formulation is proposed for predicting the efficiency of an ESP as a function of some effective parameters such as number of ionic wires and their average distance from the inlet of the ESP channel. The limitations of this formulation will be discussed in the next sections. Please note that although simulation via direct particle tracking is seemingly the most basic way to simulate an ESP process, but firstly considering the simulation speed by this method and secondly the more details of particles motion as a result of this method (the effect of engaged parameters in an ESP process might be understood in a much simpler manner and so more appropriate strategies to optimize the ESP process may follow) may be counted as the advantages/ strengths of this method over the more traditional ones.

1- Plasma Model Description and Simulation Methodology

The governing equations for corona plasma mainly consist of two conservative equations for the current and electric potential and can be solved independently of the fluid flow due to the assumption of continues phase of the fluid properties(2015) [1]. The conservative equations are as follow:

$$\nabla^2\Phi = -\frac{q_i}{\varepsilon} \quad (1)$$

$$\nabla.((b_i\nabla\Phi + \vec{U})q_i + \alpha\nabla q_i) = 0 \quad (2)$$

In which, Φ is the electric potential, q is the local space charge density, $\vec{U}$ is the fluid velocity vector, b_i is the ionic mobility in air (1.6e-4), α is ion diffusivity coefficient and ε is the electrical permittivity of the fluid.

In the present analysis, we have ignored the terms of advection by the fluid flow field and diffusion in relation to ion transport (note that the direct simulation of corona especially near the discharge surface is beyond the scope of the present work).These simplifications are based on the previous work in (2015) [1]. So the simplified form of Eq. 2 can be written as follows:

$$\nabla.((b_i\nabla\Phi)q_i) = 0 \quad (3)$$

In the present numerical simulation, the time derivative of charge field is added to the right- hand side of the Eq. 3. This transient form of the Eq. 3 leads us to the classic FTCD (Forward Time, Central Distance) discrete scheme. The reformed equation for current conservation is now written as:

$$\nabla.((b_i\nabla\Phi)q_i) = \frac{\partial q_i}{\partial t} \quad (4)$$

As it can be seen, Eq. 1 has a Poisson form for electric potential. Therefore it could be simply solved by a Gauss-Seidel scheme. Then, the calculated electric potential field is treated as a constant for the previous time step in Eq. 4. Finally, the updated charge field is substituted into the right- hand side of Eq. 1 for the next time step.

The numerical iteration continues until a steady spatial solution is achieved. The algebraic formulations for Eq. 1 and 4can be introduced based on the previous discussions as:

$$\Phi(i,j) = A\Phi(i+1,j) + B\Phi(i-1,j) + C\Phi(i,j+1) + D\Phi(i,j-1) - E\left(\frac{q^n(i,j)}{\varepsilon}\right) \quad (5)$$

$$q^{n+1}(i,j) = [Fq^n(i,j) + Gq^n(i+1,j) + Gq^n(i-1,j) + Hq^n(i,j+1) + Hq^n(i,j-1)]\Delta t + q^n(i,j) \quad (6)$$

In which, A, B, C, D and E in Eq. 5 are factors relating to the mesh structure while F, G and H in Eq. 6 are factors relating to the discrete forms for derivatives of electric potential. Note that all the spatial derivatives are approximated by second order central discrete schemes. So, this scheme includes combining the two effects of backward and forward discrete schemes for spatial derivatives in each time sweeping (interval). Although for coupled equations, a common explicit FDM algorithm is to use two middle time steps (one with backward and the other with forward discrete scheme for spatial derivatives (remind McCormack explicit procedure)) for calculating the unknowns in the next time step, but single time step method has been also used in the literature (Ex., see ref. [9]). The stability analysis of the present discrete scheme will be extensively discussed in our future work.

2- Fluid Flow Solver:

In the present numerical simulation, the fluid flow was solved using the classic Vorticity- Stream Function method which is discussed in (2016) [10]. The manipulation of the fluid flow solver consisted of a source term for plasma

and eddy- viscosity added to the molecular viscosity. In which the source term for plasma is considered to be $q_i \nabla\Phi$ and eddy- viscosity by k-ε turbulent model is discussed in the next section.

2-1 Finite Difference Approach to k-ε

For k-ε turbulent model, transport equations of kinetic energy and energy dissipation can be given by Eq. 7 and 8 respectively.

$$\frac{\partial(\rho k)}{\partial t} + div(\rho k\vec{U}) = div[\frac{\mu_t}{\sigma_k} gtad(k)] + 2\mu_t E_{ij}.E_{ij} - \rho\varepsilon \quad (7)$$

$$\frac{\partial(\rho \varepsilon)}{\partial t} + div(\rho \varepsilon\vec{U}) = div[\frac{\mu_t}{\sigma_\varepsilon} gtad(\varepsilon)] + C_{1\varepsilon}\frac{\varepsilon}{k}2E_{ij}.E_{ij} - C_{2\varepsilon}\rho\frac{\varepsilon^2}{k} \quad (8)$$

Where μ_t is the turbulent eddy- viscosity which supposed to represent the impact of unresolved velocity fluctuations of u', which is given by $\mu_t = C_\mu \rho \frac{k^2}{\varepsilon}$

E_{ij}, is the strain rate tensor in which for an incompressible flow can be given as:

$$E_{ij} = \frac{1}{2}\left(\frac{\partial u_i}{\partial x_j} + \frac{\partial u_j}{\partial x_i}\right). \quad (9)$$

The model consists of experimental constants which are described as follow:

C_μ = 0.09, σ_k =1.0, σ_ε =1.3, $C_{1\varepsilon}$ =1.44 and $C_{2\varepsilon}$ =1.92.

For the present work, we assumed the axillary parameter of $\lambda = \frac{\varepsilon}{k}$, to decouple the transport equations.

By considering $P_k = \frac{\mu_t}{2}(\frac{\partial u}{\partial y} + \frac{\partial v}{\partial x})^2$, the transport equations of k and ε for an incompressible flow can be rewritten as:

$$\frac{\partial k}{\partial t} + \nabla.(k\vec{U} - \frac{\nu_t}{\sigma_k}\nabla k) + \lambda k = P_k \quad (10)$$

$$\frac{\partial \varepsilon}{\partial t} + \nabla.(\varepsilon\vec{U} - \frac{\nu_t}{\sigma_\varepsilon}\nabla \varepsilon) + C_{2\varepsilon}\lambda\varepsilon = C_{1\lambda}P_k \quad (11)$$

Utilizing Finite Difference method by an Alternative Directional Implicit (ADI) scheme for 2D incompressible flows, the final algebraic form can be achieved.

For K transport equation, the sweep procedure in X- Direction of the channel flow can be written as:

$$(B\frac{\Delta t}{2})k^{\frac{n+1}{2}}(i-1,j) + ((A+\lambda)\frac{\Delta t}{2}+1)k^{\frac{n+1}{2}}(i,j) - B\frac{\Delta t}{2}k^{\frac{n+1}{2}}(i-1,j) = k^n(i,j) + \frac{\Delta t}{2}Ck^n(i,j+1) - Ck^n(i,j-1) + \frac{\Delta t}{2}P_k \quad (12)$$

For K transport equation, the sweep procedure in Y- Direction of the channel flow can be written as:

$$(C\frac{\Delta t}{2})k^{n+1}(i,j-1) + ((A+\lambda)\frac{\Delta t}{2}+1)k^{n+1}(i,j) - C\frac{\Delta t}{2}k^{n+1}(i,j+1) = k^{\frac{n+1}{2}}(i,j) + \frac{\Delta t}{2}Bk^{\frac{n+1}{2}}(i+1,j) - Bk^{\frac{n+1}{2}}(i-1,j) + \frac{\Delta t}{2}P_k \quad (13)$$

The same routine could be pursued for ε transport equation, and then the sweep procedure in X- Direction of the channel flow can be written as:

$$(B\frac{\Delta t}{2})\varepsilon^{\frac{n+1}{2}}(i-1,j)+([A+C_{2\varepsilon}\lambda]\frac{\Delta t}{2}+1)\varepsilon^{\frac{n+1}{2}}(i,j)-B\frac{\Delta t}{2}\varepsilon^{\frac{n+1}{2}}(i-1,j)=\varepsilon^{n}(i,j)+\frac{\Delta t}{2}C\varepsilon^{n}(i,j+1)-C\varepsilon^{n}(i,j-1)+\frac{\Delta t}{2}C_{1\varepsilon}\lambda P_k \quad (14)$$

And finally for ε transport equation, the sweep procedure in Y- Direction of the channel flow can be written as:

$$(C\frac{\Delta t}{2})\varepsilon^{n+1}(i,j-1)+([A+C_{2\varepsilon}\lambda]\frac{\Delta t}{2}+1)\varepsilon^{n+1}(i,j)-C\frac{\Delta t}{2}\varepsilon^{n+1}(i,j+1)=\varepsilon^{\frac{n+1}{2}}(i,j)+\frac{\Delta t}{2}B\varepsilon^{\frac{n+1}{2}}(i+1,j)-B\varepsilon^{\frac{n+1}{2}}(i-1,j)+\frac{\Delta t}{2}C_{1\varepsilon}\lambda P_k \quad (15)$$

In Eq. 16 to 19, the factors of A, A', B and C are defined as follow:

$$A=2\frac{\mu_t}{\sigma_k}(\frac{1}{\Delta x^2}+\frac{1}{\Delta y^2}) \quad (16)$$

$$A'=2\frac{\mu_t}{\sigma_\varepsilon}(\frac{1}{\Delta x^2}+\frac{1}{\Delta y^2}) \quad (17)$$

$$B=\frac{-u}{2\Delta x}+\frac{\nu_t}{\Delta x^2} \quad (18)$$

$$C=\frac{-v}{2\Delta y}+\frac{\nu_t}{\Delta y^2} \quad (19)$$

Where u and v are the solved velocities in X and Y directions respectively. Eq.12 to 15 are solved using TDMA while in each time step, the values of λ and μ_t must be updated.

To update eddy viscosity and auxiliary parameter of λ, the following procedure was pursued as discussed in the previous work by authors [11].

Since eddy viscosity is limited by a certain fraction of molecular viscosity near the walls and its maximum value of $\nu_{t\max}=l_{\max}\sqrt{k}$ (where $l_{\max}$ is the maximum certifiable mixing length, which represents the largest size of eddies that can be considered as the width of the domain), the limited mixing length can be defined as $l_l=C_\mu\frac{k^{1.5}}{\varepsilon}$ if $C_\mu k^{1.5}<\varepsilon l_{\max}$ or $l_{\max}$ if otherwise. Then eddy viscosity can be quantified as $\nu_t=\max(\nu_{t\min},l_l\sqrt{k})$ and finally, the auxiliary parameter of λ is then updated to $\lambda=C_\mu\frac{k}{\nu_t}$.

2-2 Boundary Condition for k-ε Turbulent Model:

Boundary conditions for k-ε turbulent model were implemented also based on our previous work [11].

For inlet condition, the value for k and ε can be assumed as:

$$k=\xi U_\infty^{\,2} \quad (20)$$

$$\varepsilon=\frac{k^{\frac{3}{2}}}{0.1\delta} \quad (21)$$

Where ξ is a constant that is assumed to be 0.01 in the present work and δ is the half of the modeled channel flow.

For walls condition, the value for k and ε is assumed as:

$$k=0 \quad (22)$$

$$\varepsilon=2\nu\frac{d}{dy}\sqrt{k} \quad (23)$$

For outlet condition, the value for k and ε is calculated by the following Dirichlet boundary conditions:

$$\frac{\partial k}{\partial x} = 0 \quad (24)$$

$$\frac{\partial \varepsilon}{\partial x} = 0 \quad (25)$$

3- Particle Tracking, Particle Charge and Peek Law Condition

For tracking a particle (particulate matter that must be removed through the ESP process), we followed the same governing Lagrangian equation which was presented in (2007) [2]. This equation considers the aerodynamic forces (created by the viscous effects), columbic forces and the gravity on a particle. Although by simply using DPM (Discrete Phase Model) code which is available in some commercial softwares, the concentration distribution of the repositioned particles will be achieved, but in the present simulation, in order to only deal with the Lagrangian parameters (note that particle concentration is an Eulerian parameter and the main goal of the present work is to disclose a direct particle tracking scheme), we tracked a finite number of particles from the inlet of the ESP channel to the outlet in order to only focus on particles fate in individual. This procedure will lead us to a better understanding of what truly happens on a single particulate matter when it is confronted to several external forces including columbic and aerodynamics through an ESP channel. The governing equation on particles motion can be written as follows:

$$\frac{d\vec{u}_{p,i}}{dt} = F_D(\vec{u}_i - \vec{u}_{p,i}) + \frac{g_i(q_p - \rho)}{q_p} + \vec{F}_i \quad (26)$$

As it can be seen from Eq. 26, the effect of Brownian motions has been neglected. Furthermore, we must have a scheme for simulating the interactions of particles to each other and also to the grounded collector plate. In the case of particles with smaller sizes, it is deciphered that they might be absorbed while impacting to each other. So there would be a diffusivity factor for each impact at least relating to the specific angle of impact and particles properties. Moreover, treating with particles when they meet the wall surface requires Monte Carlo methodology for a more exact simulation. So a full simulation of particle trajectory with considering the whole effects, takes a long time consuming numerical path. So in this work by some simplifying assumptions, we have reduced the ESP complex phenomena into a simpler one.

Treating the impact of ash particles as solids dynamical interaction requires to define the diffusivity factor ($0 < \varepsilon = \left|\frac{V_2' - V_1'}{V_2 - V_1}\right| < 1$).In a more detailed point of view, this factor varies between 0 and 1. In which"1" represents that, the speed gradient of particles does not change after the impact. Besides, "0" indicates that the two particles might be attached after the impact. This factor mainly depends on several parameters including the properties of particles, the speed of particles (this parameter is related to the fluid's velocity), angle of attack and etc.; while assuming this factor as to be "1" ($\varepsilon = 1$)seems convincing in higher Reynolds numbers for some particular particles. The effect of dynamical impact should be applied when the path lines of particles meet each other. Including the impact effects simply interrupts the validity of the assumption of a constant time scale in the numerical procedure; because this impact might occur in a smaller time scale than what which is set in the numerical procedure. Therefore, as a simplifying assumption in the present work, the particles path line could meet each other without effecting on their trajectories. We later discuss that this assumption may not considerably affect the outcome results.

We have further assumed that a particle which is so close to the collector surface is absorbed by the surface. An additional assumption was to ignore the gravity force with respect to the magnitude of other external forces on a particle (these assumptions are also common in DPM simulation).

Particles obtain a value of charge when they are floating into the media of the ionized gas. This value of charge stands as a function of particle diameter (particles are assumed to have spherical form), relative permittivity of gas, electric field and the resident time for particles in the computational cell (this resident time in computational cell is transformed in meaning into the resident time of the particles in four surrounding grids that represent a specific cell). Particle charge can be defined by Pauthenier equation (2007) [2] as follows:

$$q_p = \left[1 + 2\left(\frac{\varepsilon_r - 1}{\varepsilon_r + 1}\right)\right] 4\pi {r_p}^2 \varepsilon_0 \left|\vec{E}\right| \frac{t}{(t + \tau)} \quad (27)$$

Peek law condition is applied to predict the charge density at the discharge electrode and this boundary condition is updated at each time step. The charge density at discharge electrode is defined as:

$$\rho_0 = -\frac{\varepsilon(E - E_0)}{ds} \tag{28}$$

E_0 in Eq. 28 is obtained using peek law condition:

$$E_0 = E_{Peek} = 3.1\times10^6 \delta(C_1 + C_2/\sqrt{\delta r}) \tag{29}$$

Eq. 26 to 29, are well specified in [2] and were solved in this research by using forward time discrete scheme.

4- ESP Geometry, Boundary Conditions and Properties of Particulate Matters

In this section, the particle properties for ash as the particulate matter, applied voltage and current for wires and flow conditions at the boundaries are specified. The geometry and conditions that we applied in the present simulation are shown in Fig. 1. Note that in the present study, we changed the arrangement of wires in each studied case. So Fig. 1indicatesthe schematic and conditions that were generally applied in the present work.

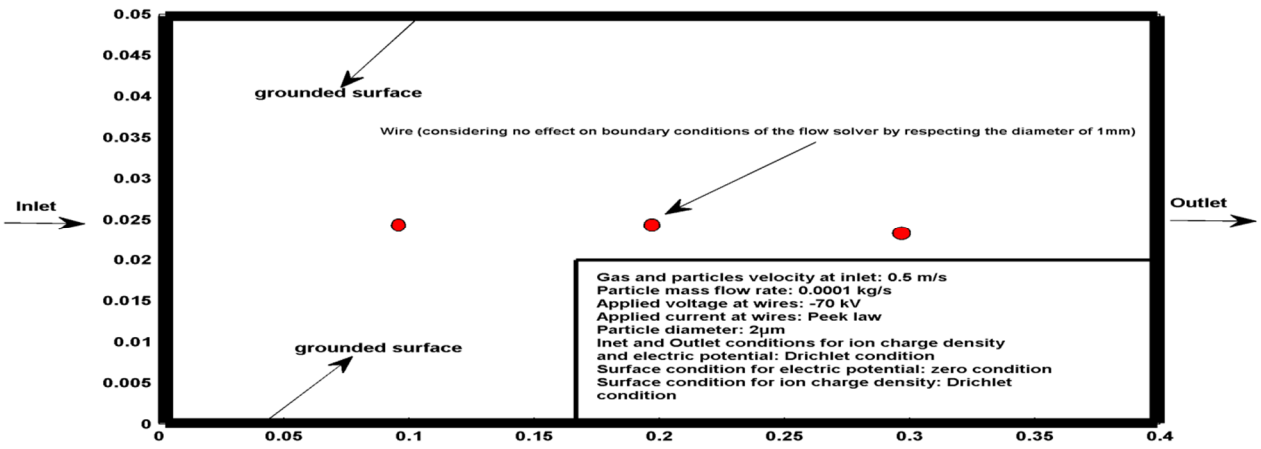

Fig. 1 Schematic and conditions of the problem (distances are assumed to be in SI unit)

5- Numerical Results and Discussion

The results of this research are divided into two sections. First, the results for applying three different arrangements of wires (one, two and three number of wires with a certain distance to each other) are shown and discussed after validating the turbulent model and corona plasma wind. In the next section, by continuing the procedure of simulation for many different cases (wires with different arrangements), a formulation is proposed for ESP efficiency as a function of number of applied wires and their average distance from the inlet. As it was discussed earlier, this correlation which is based on numerical results of many cases can be beneficial for primary calculations for industrialization of an ESP.

5-1 First Section of Results

To start further discussion, it is worth to note that some criteria have been reported so far that represent the electro-hydrodynamic impact on the fluid flow; so we have picked one to see whether this impact is negligible or not. Coming to this point that IEEEDEIS- EHD Technical Committee has proposed that the significant EHD effects can happen if $Md > Re_L^2$ (these factors are well defined in [1]).It was calculated that for the present study, Md is more than 20 times smaller than Re_L^2. Then it is simply concluded that EHD (Electro- Hydro- Dynamic) impact on the fluid flow is negligible. Noting that there are several phenomena engaged with the ESP process that require a time consuming numerical path, for the current numerical simulation, we applied one more simplification. Based on this simplification, particle tracking process was followed by setting a time step in which allowed the particles to skip from at the most three cells in each iteration process. Although this simplification brings some errors (including the interruption of resident time for particle charge), but the out- coming results were still in a good agreement with the previous works in this field. Since we have considered a finite number of particulate matters entering the channel (each cell at the inlet of the channel acquires one particle), then we have already assumed that the numerous particles inside a specific computational cell in a real ESP channel, have relatively similar behavior.Following the

discussions presented so far in this study, the ESP efficiency in collecting the particulate matters can be simply defined by the following relation.

$$e\% = \frac{N_{Collected}}{N_{Inlet}} \times 100 \quad (30)$$

In Eq. 30, $N_{Collected}$ is the number of collected particles and N_{Inlet} is the number of particles that are assumed at the inlet of the ESP channel.

Here we discuss a situation in which the particles interaction is to be included:

Note that different concentrations of particulate matters at the inlet while having other geometrical parameters and ESP properties constant, may result in relatively different ESP efficiency in collecting the particles (the assumption of considering one particle inside each computational cell at the inlet, means that the many particles in each cell (in a real ESP channel) have similar behaviors). So, there would be a weakness in the present numerical procedure. Because a higher particle concentration at the inlet will be simulated just as the way of simulating lower concentrations by assuming one particle in each computational cell at the inlet. Then the present simulation procedure needs a complementary relation which indicates the number of particles that are required to be assumed in one cell at the inlet that corresponds to the effects of particles concentration on particles interaction. Although having the need for a complementary relation answered, requires further researches, but even by ignoring the particle interactions we have still seen a good agreement with the previous work in (2006) [3]. Three ionic wired ESP channel with the conditions of d_p= 2μm, wire voltage= 70kV, concentration= 1 g/m^3, gas and particle velocity at inlet= 1.0 m/s has been simulated in [3]. The ESP efficiency in removing the particulate matters of ash was calculated and compared to that of the previous study (see ref. (2006) [3]). In this case, the deviation in ESP efficiency was about 4%. Therefore, as previously discussed, the present approach may be considered as an alternative to more traditional approaches in simulating ESP process.

Coming to convergence of the present approach, it should be mentioned that Eq. 26 can be mainly described as:

$$f'(t) = Af(t) + B \quad (31)$$

In which, A and B are spatial factors (A= g(x, y) and B= h(x, y)). So by using the traditional forward Euler algorithm (forward time discrete scheme), the convergence would be only reliant on the convergence of fluid flow solver (including turbulent effects) and plasma solver which were previously discussed.

Main results of the present numerical simulation are presented in Fig. 2 to Fig. 11; in which the validity of corona plasma wind is compared to the previous work in [2] and shown in Fig. 2; Fig. 3indicates the fully- developed turbulent velocity profile; Fig. 4 to Fig. 6 betray the validation for u^+ and turbulent characteristics of u_{rms} and v_{rms} with the previous work by Kim et al. for Reynolds number of 5600(see ref. (2016) [12]).Fig. 7 shows the electric field of the corona plasma in a contour form. From Fig. 7, it can be seen that the electric fields decays rapidly by getting far from the ionic wires. Fig. 8shows the electric field vectors which are defined as: $\vec{E} = -\nabla\Phi$. Fig. 9 to Fig. 11indicate the finite number of particles tracked through the ESP channel. In which, one, two and three ionic wires were applied in Fig. 9, 10 and 11 respectively (note that these figures represent the converged results which was found in using 46 particles at the inlet of the ESP channel). As it can be seen from these figures, we have particles interaction only in Fig. 9 which only one ionic wire was applied. This happens, because of the behavior of Eq. 26. As a more detailed discussion, the reason for this interaction may be explained by this way that when we have only one ionic wire, there would be a relatively lower vertical force (which is directed to the grounded plates) on the particles. This force is mainly due to the Columbic force of ionic wires (see Fig. 8). So, as the maximum of y-component velocity occurs just near the wall at the inlet of ESP channel, this discrepancy might be already anticipated in this region. With the increase of ionic wires, there is no particles interaction and particles almost follow a curve- like trajectory to the grounded plates (see Fig. 10 and 11). Since by ignoring the particles interaction effect, each particle path line behaves independently than the others, tracking lower number of particles only results in eliminating the remaining path lines from these figures (Fig. 9 to 11). For a simple ESP channel (which the fluid flow is almost one- dimensional) with the boundary conditions used in this work and ash properties, the present approach seems promising. Generally, if particles interaction is to be ignored, the simulation procedure should be continued by increasing the number of particles until the efficiency of ESP in removal of particulate matter converges; yet considering particles interaction brings some more complexities to the problem (as previously discussed) and resolving this issue is in progress by authors. As a gist, the convergence of the efficiency of ESP in removal of the particles is summarized in Table. 1for the case of three ionic wires. In order to illustrate the above discussion, the results for three ionic wires and 22 particles is shown in Fig. 12. As previously mentioned, Fig. 12 is relatively similar to Fig. 11.

Table 1. Independency of ESP efficiency from number of particles for the case of three ionic wires

Number of Particles	Efficiency of ESP %
10	80
22	72
30	66
36	66
42	65
46	65

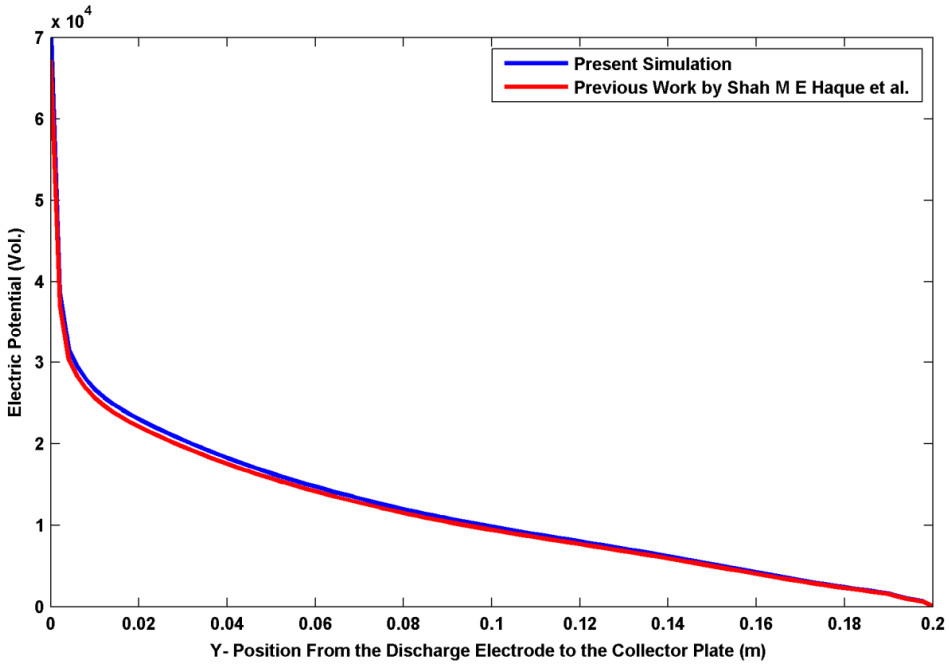

Fig. 2 The distribution of electric potential

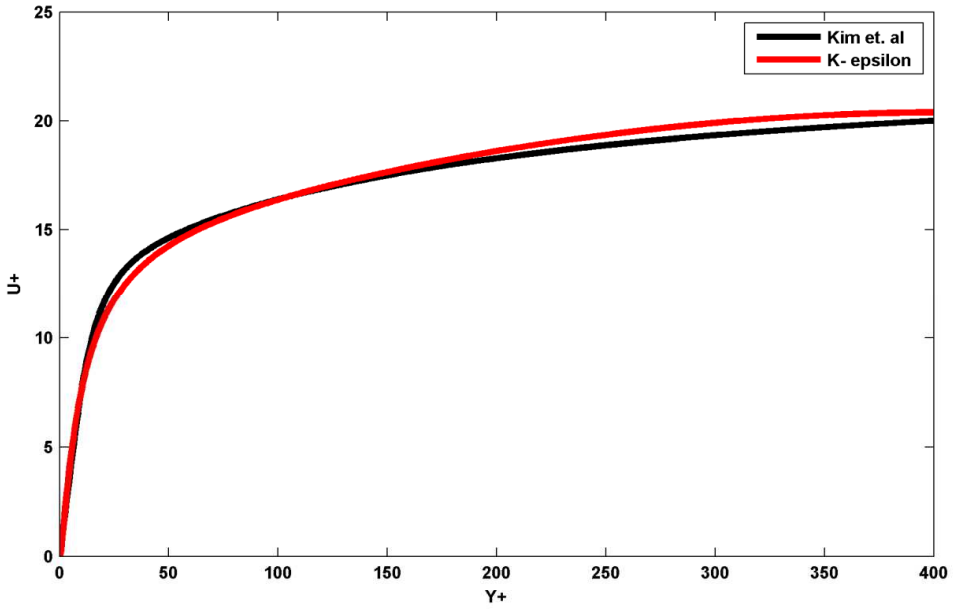

Fig. 3 u^{n}measured to the half of the ESP channel

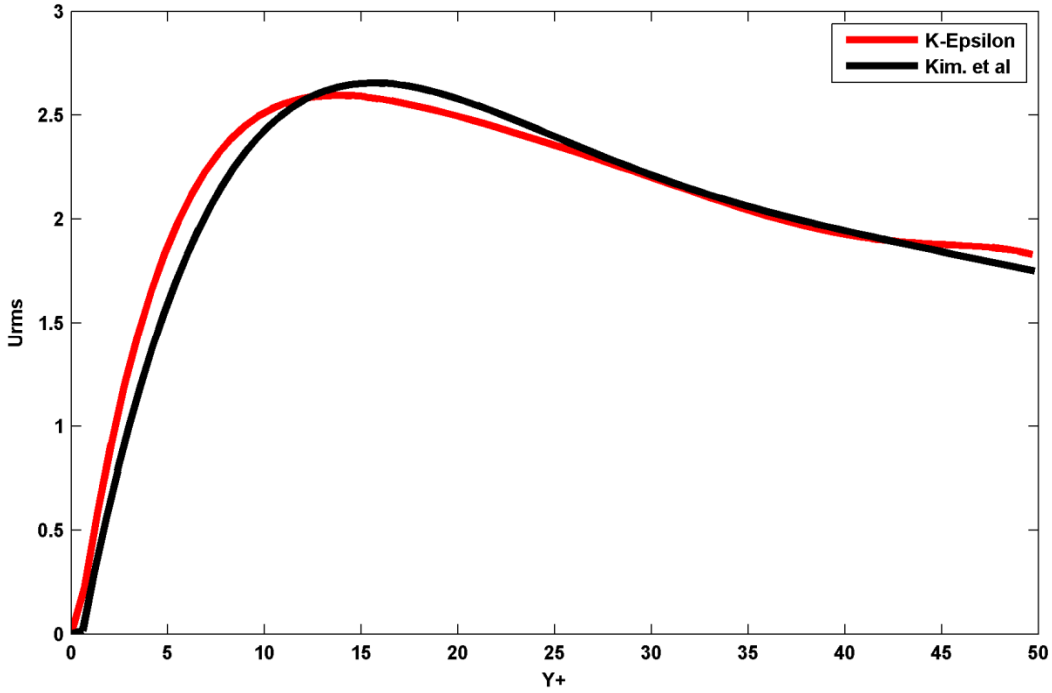

Fig. 4 u_{rms} to y+ of 50 in the ESP channel

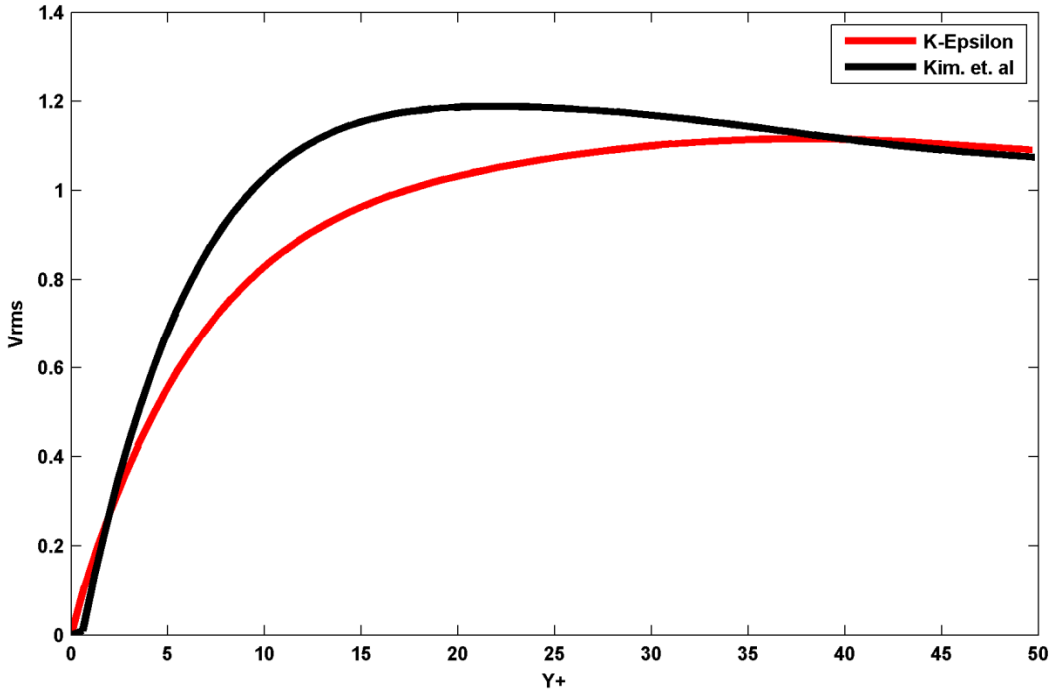

Fig. 5 v_{rms} to y+ of 50 in the ESP channel

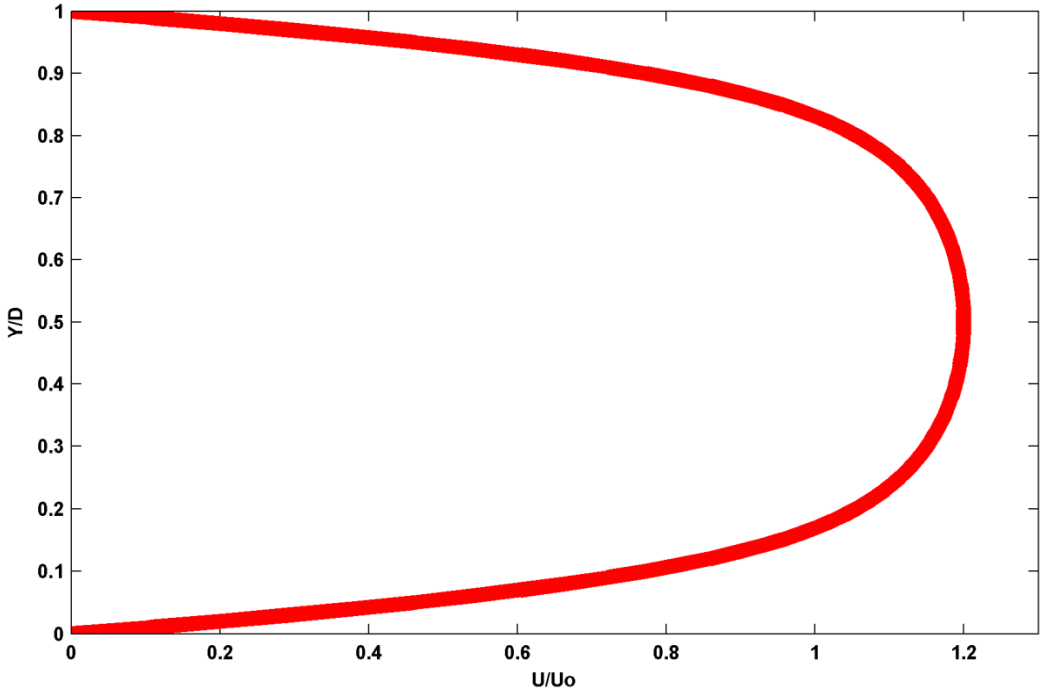

Fig. 6 Fully- developed velocity profile in the ESP channel under a turbulent flow regime

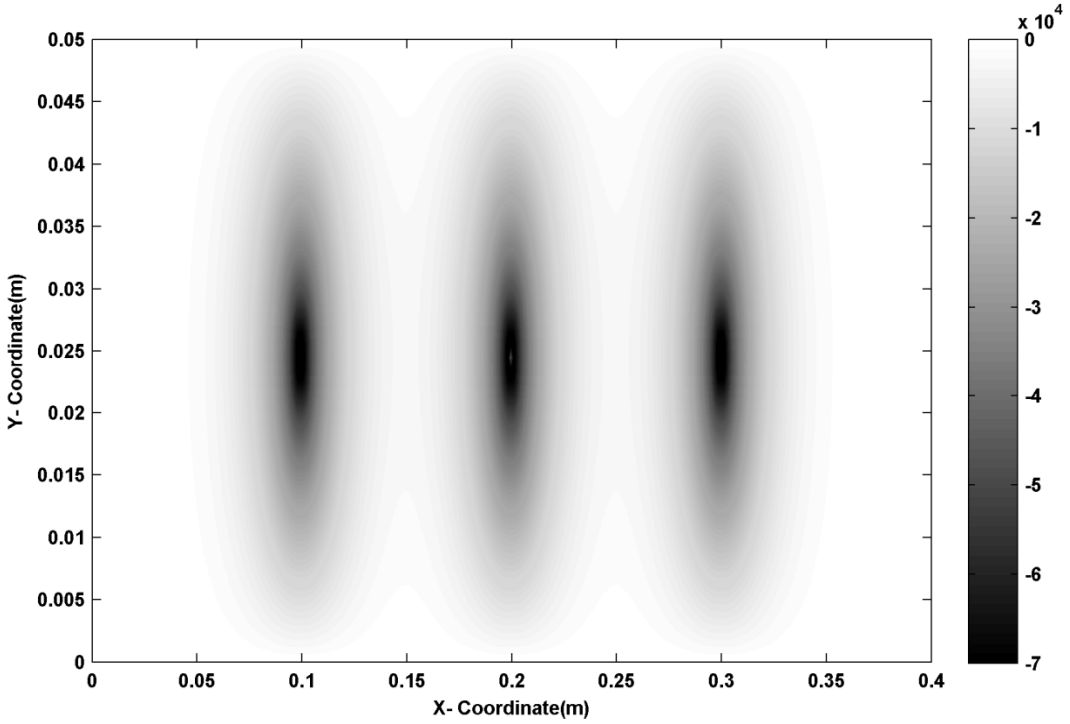

Fig. 7 Electric potential contour inside the ESP channel

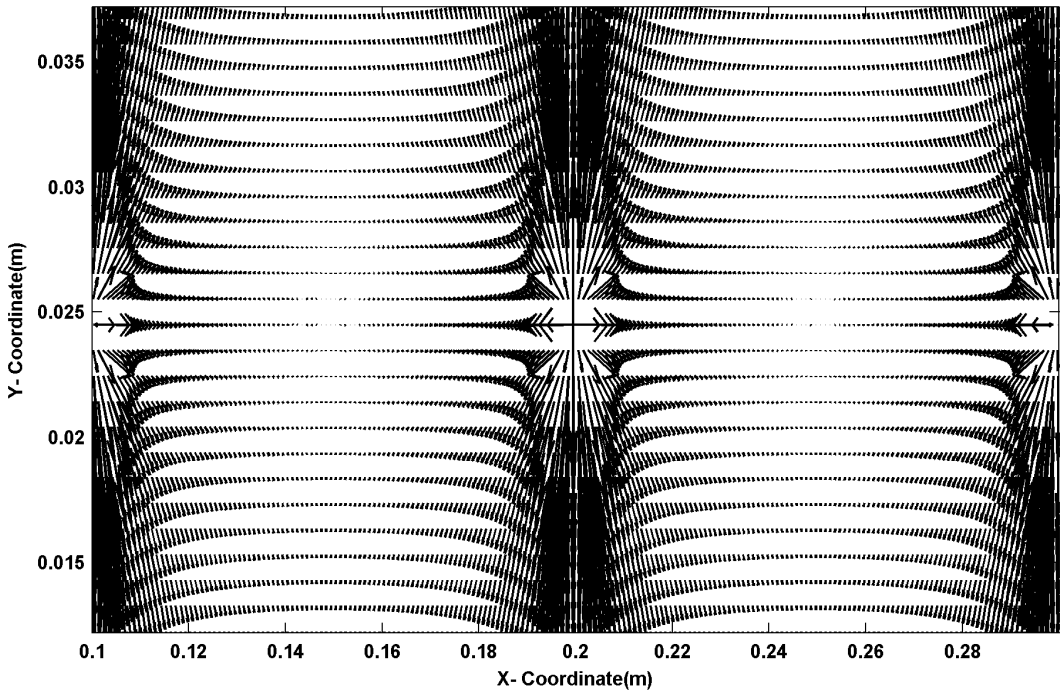

Fig. 8Zoomed in view of the electric field vector ($\vec{E} = -\nabla\Phi$) inside the ESP channel

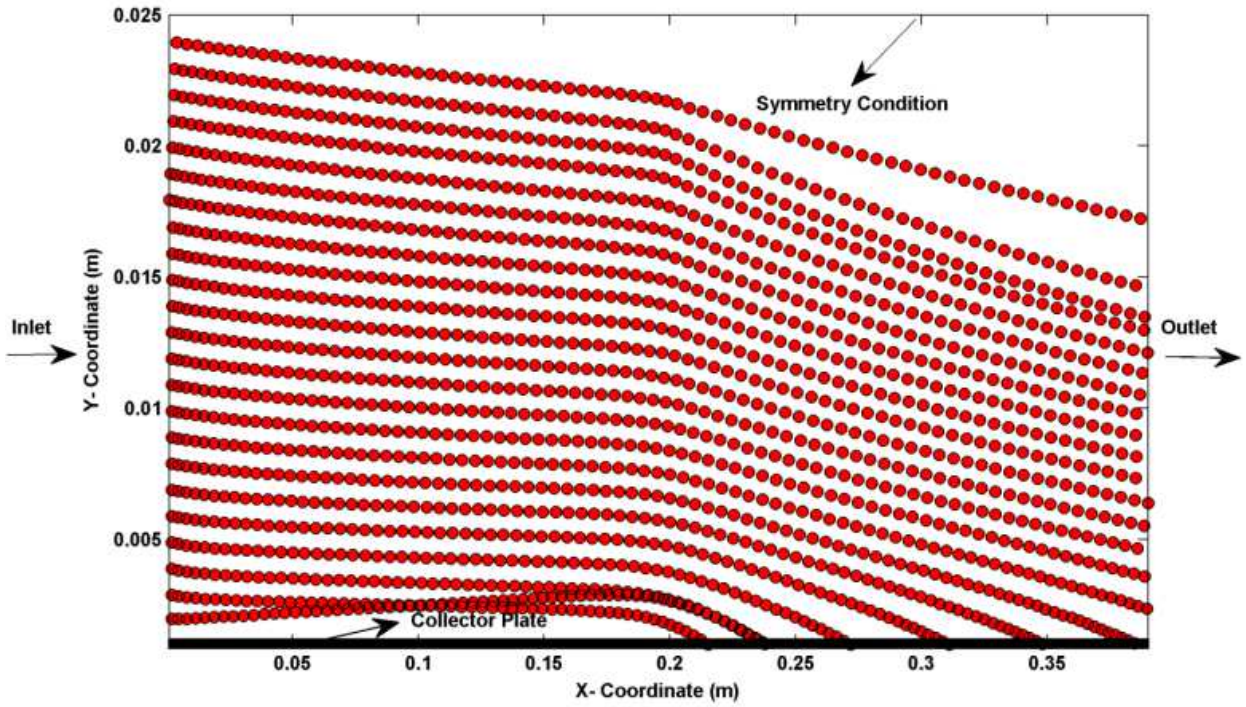

Fig. 9 Particle tracking from the inlet to the outlet of the ESP channel (half of the channel is shown for one applied wire at the coordinate of x= 0.1 m and y= 0.025 m): 46 particles tracked

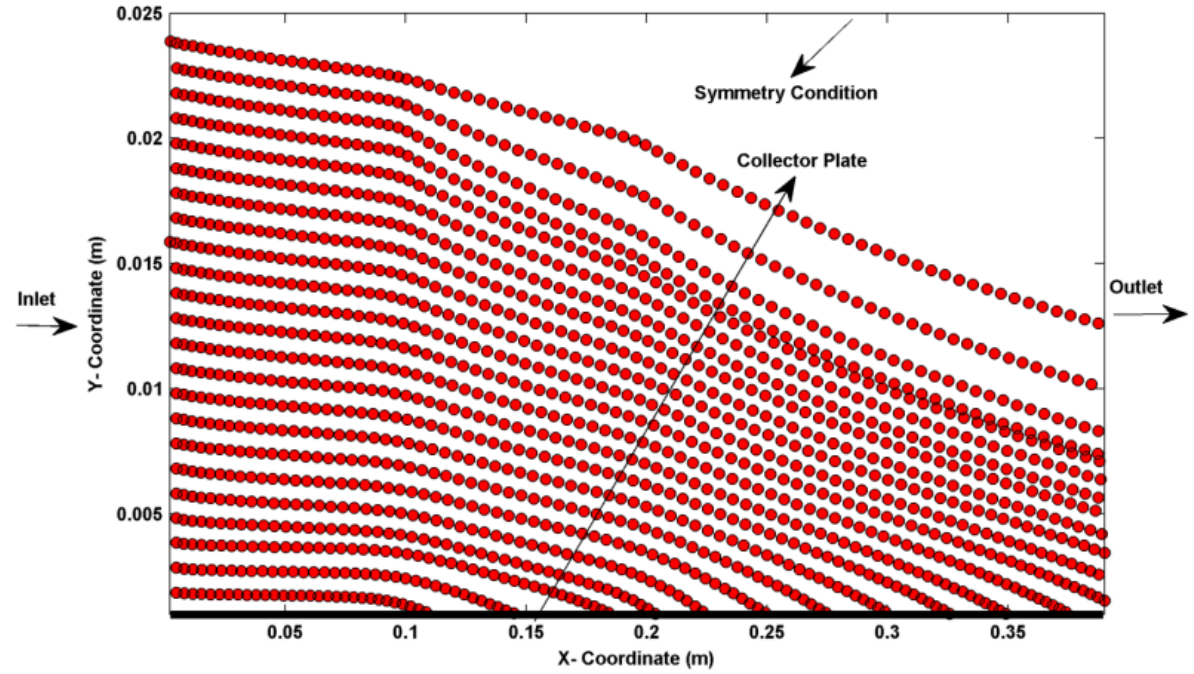

Fig. 10 Particle tracking from the inlet to the outlet of the ESP channel (half of the channel is shown for two applied wires at the coordinates of x= 0.1 m, y= 0.025 m and x=0.2 m, y=0.025 m): 46 particles tracked

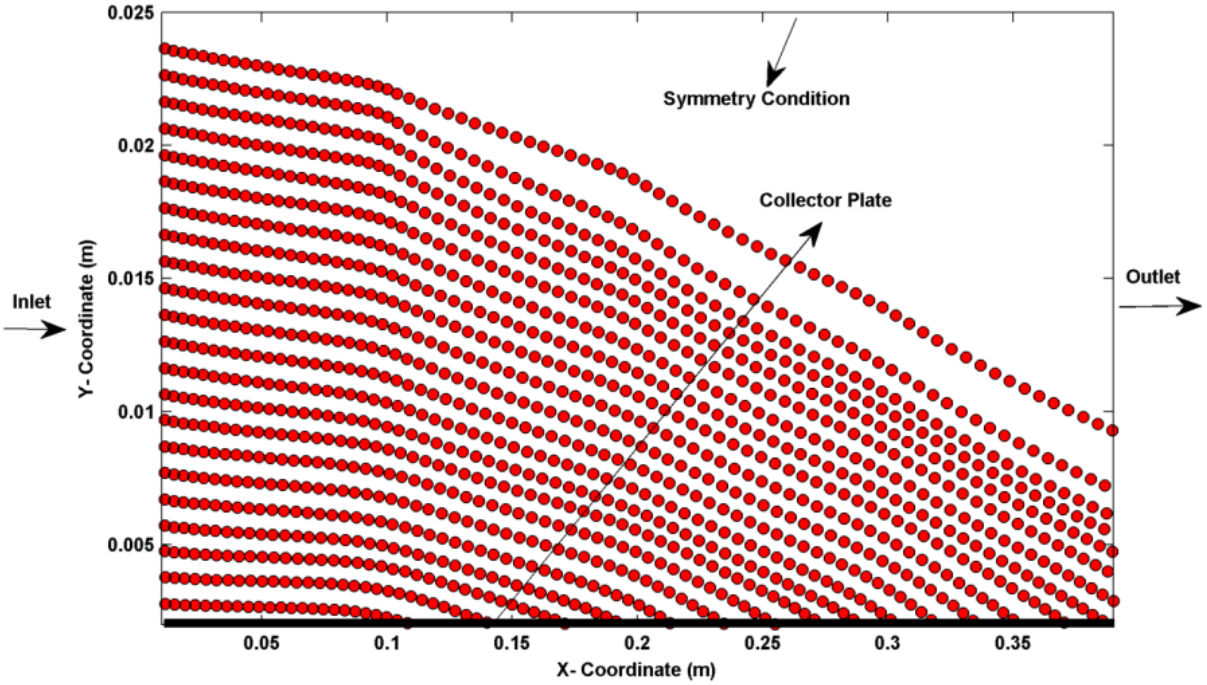

Fig. 11 Particle tracking from the inlet to the outlet of the ESP channel (half of the channel is shown for three applied wires at the coordinates of x= 0.1 m, y= 0.025 m; x=0.2 m, y=0.025 m and x=0.3, y=0.025 m): 46 particles tracked

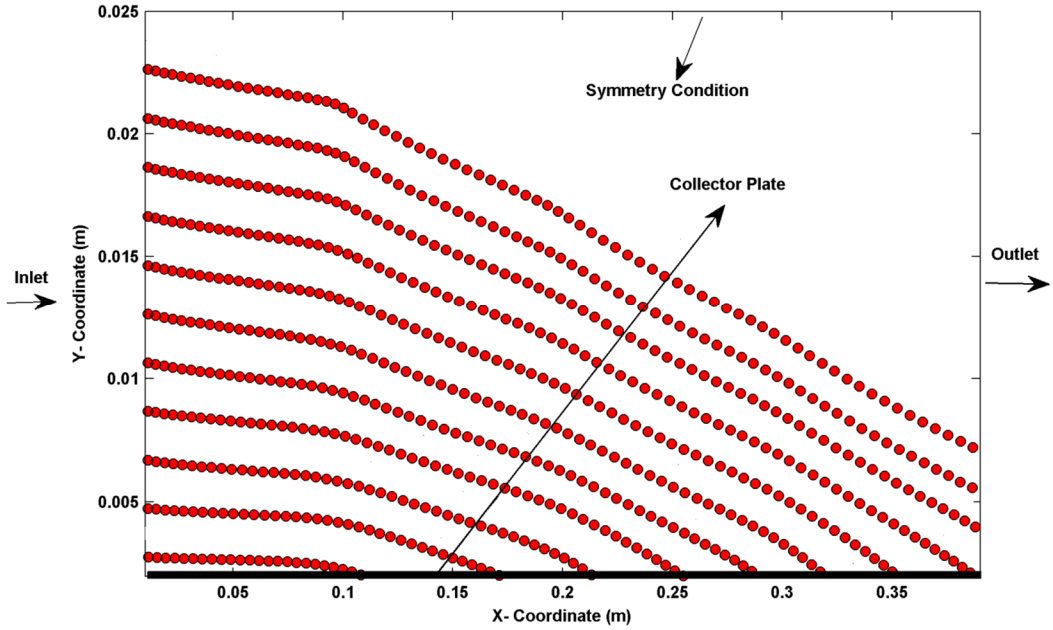

Fig. 12 Particle tracking from the inlet to the outlet of the ESP channel (half of the channel is shown for three applied wires at the coordinates of x= 0.1 m, y= 0.025 m; x=0.2 m, y=0.025 m and x=0.3, y=0.025 m): 22 particles tracked

5-2 Second Section of Results

The numerical simulation was continued for variety of ESP cases in which we kept the geometry of the ESP channel and also the electrical conditions of wires constant, while the number of wires and their average distance from the inlet were altered. The results of studied cases are collected in Table. 2. Finally using Least Square Regression Optimization (2016) [12- 15], a correlation was derived for estimating the ESP efficiency in particulate matter removal.

$$e\% = 12.1 + 22.5n - 71.9d \quad \text{(R-Square ~0.99)} \qquad (32)$$

Where, e% is the efficiency of the ESP channel which was defined previously, "n" is the number of ionic wires (natural values) and "d" is their average distance from the inlet of the ESP channel. This correlation is valid for natural values of "n" (indicator of the number of applied wires) top to 3 and the average distance of wires from the inlet("d") top to 0.4m. As it can be seen from Table. 2, in each certain number of applied wires, efficiency decreases with the increase of average distance from the inlet. Moreover, efficiency increases with the increase of number of applied wires in each certain average distance from the inlet. Combining these two previous statements, the maximum of ESP efficiency in particulate matter removal was found in the case of three ionic wires with the average distance of 5cm from the inlet. These results can be physically justified in this way that by decreasing the average distance, the particles will be rapidly affected by the electric field of wires. So, their path lines bend quickly to the grounded plates. Therefore, the probability to impact to the grounded surfaces increases. Here, it is worth to note that the concept of average distance from the inlet is rather doubtful; because the position of each ionic wire in individual affects the efficiency. Furthermore, the present formulation is only valid for the conditions used in this work. So, developing a more general formulation is in progress.

Table 2 The results of studied cases

N	d	e%	N	d	e%	N	d	e%
1	0.05	31	2	0.05	54	3	0.05	76
1	0.1	26	2	0.1	51	3	0.1	71
1	0.15	21	2	0.15	48	3	0.15	67
1	0.2	19	2	0.2	46	3	0.2	65
1	0.25	17	2	0.25	41	3	0.25	59
1	0.3	13	2	0.3	39	3	0.3	57
1	0.35	9	2	0.35	37	3	0.35	55

Conclusion

In this study, the ESP (Electro- Static Precipitator) was simulated by a rather simple and fast Finite Difference approach. This simulation allows us to directly track the particulate matters to their fates. Since the previous methodologies were almost relied on an Eulerian demonstration of the particle tracking (providing the concentration of particles through the ESP process), the present work focuses on pursuing a finite number of particles to their fates. Considering that the numerous particles in a specific computational cell, behave similar to each other, this methodology stands as a fast simulation to track the particulate matters inside an ESP with a fully- Lagrangian aspect. Although the numerical procedure contains some simplifications but the outcome results were still reliable. The method deals mostly with ratio of the trapped particles but since particles interaction is a complex phenomenon and also includes an external dynamical pattern, it cannot be simply concluded that different concentrations of particulate matters at the inlet of the ESP channel will result in a same ratio of the trapped particles. Although the particles interaction was not included in the present simulation, but for including this effect, we hypothesize that there is a direct relation between the number of particles which is needed to be assumed in each computational cell at the inlet and the particles concentration at the inlet, to reach precise results for any desired concentration of particulate matter at the inlet of the ESP channel. Having this that there are many of factors that affect the ESP efficiency (including inlet Reynolds number, ESP length, the number of applied wires, the distance between these wires, electrical parameters of wires, and so forth for a classical ESP scheme), a correlation was proposed for the ESP efficiency in removing the particulate matters (which was considered to be ash in this work) as a function of the number of applied wires and their average distance from the inlet of the ESP channel. Although as discussed, this correlation is not applicable for many other ESP configurations, but it reveals some important facts about the effects of two parameters on a classical ESP model. Finally it is worth to say that this methodology that was extensively introduced in this study, is recommended for fast and primary calculations of ESP process. In further works, authors will aim to resolve the limits from the present approach.

REFERENCES

[1] Herek L. Clack, Simultaneous Removal of Particulate Matter and Gas-Phase Pollutants within Electrostatic Precipitators: Coupled In-Flight and Wall-Bounded Adsorption, Aerosol and Air Quality Research, 15: 2445–2455, 2015 Copyright © Taiwan Association for Aerosol Research ISSN: 1680-8584 print / 2071-1409 online, doi: 10.4209/aaqr.2015.04.0280

[2] Shah M E Haque1, M G Rasul, M M K Khan, A V Deev1, and N Subaschandar1, A Numerical Model of an Electrostatic Precipitator, 16th Australasian Fluid Mechanics Conference Crowne Plaza, Gold Coast, Australia 2-7 December 2007

[3] G. Skodras, S.P. Kaldis, D. Sofialidis, O. Faltsi, P. Grammelis, G.P. Sakellaropoulos, Particulate removal via electrostatic precipitators — CFD simulation, Fuel Processing Technology 87 (2006) 623–631

[4]L. ZHAO, E. DELA CRUZ, K. ADAMIAK, A.A. BEREZIN, J.S. CHANG, A NUMERICAL MODEL OF A WIRE-PLATE ELECTROSTATIC PRECIPITATOR UNDER ELECTROHYDRODYNAMIC FLOW CONDITIONS, ICESP X – Australia 2006 Paper 7B3

[5] H E R E K L. C L A C K. Particle Size Distribution Effects on Gas-Particle Mass Transfer within Electrostatic Precipitators, Environ. Sci. Technol. 2006, 40, 3929-3933

[6] Niloofar Farnoosh. Three-Dimensional Modeling of Electrostatic Precipitator Using Hybrid Finite Element – Flux Corrected Transport Technique, 2011, Electronic Thesis and Dissertation Repository, the University of Western Ontario

[7] Muhammad Ahmad and Jhanzeb, Modeling and Simulation of an Electrostatic Precipitator, School of Computer Science, Physics and Mathematics Växjö, 2011, Sweden.

[8] Clack, H.L. (2009). Mercury Capture within Coal-fired Power Plant Electrostatic Precipitators: Model Evaluation. Environ. Sci. Technol. 43: 1460–1466.

[9] DM Orlov, Modelling and Simulation of Single Dielectric Barrier Discharge Plasma Actuators [Dissertation]. Notre Dame, Indiana, University of Notre Dame, 2006.

[10] Aberoumand, S., Jafarimoghaddam, A. and Aberoumand, H. (2016), Numerical Investigation on the Impact of DBD Plasma Actuators on Temperature Enhancement in the Channel Flow. Heat Trans. Asian Res.. doi: 10.1002/htj.21227

[11]A Jafarimoghaddam and S Aberoumand, the Impact of DBD Plasma Actuator on Turbulent Characteristics in the Channel Flow: A Comparison between Two RANS Models by Finite Difference Approach, European Journal of Advances in Engineering & Technology, 2016, 3 (8), 13-20.

[12] J. Kim, P. Moin, R. Moser, "Turbulence statistics in fully developed channel flow at low Reynolds number" NASA Ames Research Center, Moffett Field, CA 94035, USA.

[13] Jafarimoghaddam, A., Aberoumand, S., Aberoumand, H. and Javaherdeh, K. (2016), Experimental Study on Cu/Oil Nanofluids through Concentric Annular Tube: A Correlation. Heat Trans. Asian Res.. doi: 10.1002/htj.21210

[14] A. Jafarimoghaddam, S. Aberoumand, An empirical investigation on Cu/Ethylene Glycol nanofluid through a concentric annular tube and proposing a correlation for predicting Nusselt number, Alexandria Eng. J. Volume 55, Issue 2, June 2016, Pages 1047–1052

[15] Sadegh Aberoumand, Amin Jafarimoghaddam, Mojtaba Moravej, Hossein Aberoumand, Kourosh Javaherdeh, Experimental study on the rheological behavior of silver- heat transfer oil nanofluid and suggesting two empirical based correlations for thermal conductivity and viscosity of oil based nanofluids, Applied Thermal Engineering, Volume 101, 25 May 2016, Pages 362–372.

[16] A. Jafarimoghaddam, S. Aberoumand, A Least Squares Regression Formulation for Dielectric Barrier Discharge (DBD) Plasma Actuator Body Force by Scrutinizing the Lumped Circuit Element Electro- Static Model: A Short Report, J. Appl. Environ. Biol. Sci., (2107), Vol. 7, No. 1.